

Concepts for Experiments at Future Colliders I

PD Dr. Oliver Kortner

05.02.2024

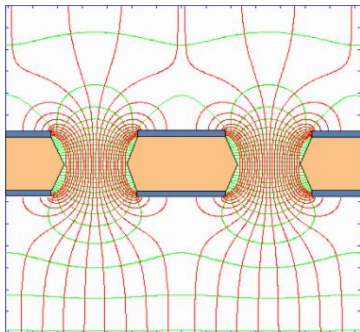
Micropattern gaseous ionization detectors

- The charge particle detection efficiency of a detector under high particle background is given/determined by the size of its active "space-time" area, i.e. its spatial granularity and its dead time.
- Micropattern gaseous ionization detectors are fast gaseous ionization detectors with high spatial granularity for the operation in high background environments.
- Most prominent examples: GEMs, MicroMegas.

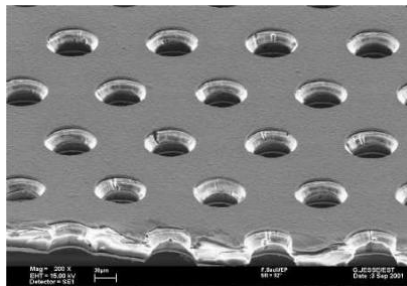
Recapitulation of the previous lecture

Gas Electron Multiplier (GEM)

- The heart of a GEM is a thin, metal-clad polymer foil, chemically pierced by a high density of holes (typically 50 to 100 per mm^2). On application of a difference of potential between the two electrodes, electrons released by radiation in the gas on one side of the structure drift into the holes, multiply and transfer to a collection region.



Field lines and equipotentials in the GEM holes on application of a voltage between the two metal sides. A drift (top) and transfer (bottom) field transport ionization electrons into and out of the holes.



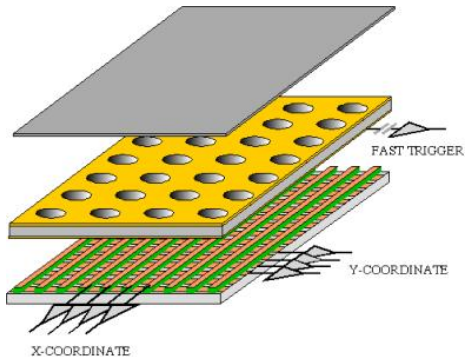
Close view of a GEM electrode, etched on a metal-clad, 50 μm thick polymer foil. The hole's diameter and distance are 70 μm and 140 μm .

Recapitulation of the previous lecture

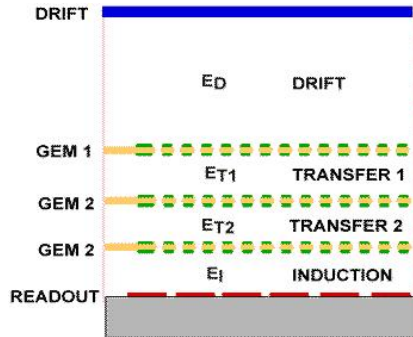
Single and multiple GEMs

Schematics of a single GEM detector.

Electrons released by ionization in the top gas volume drift and multiply in the holes; the charge is collected on the anode, with 1-D or 2-D projective strips, pads or other patterns.

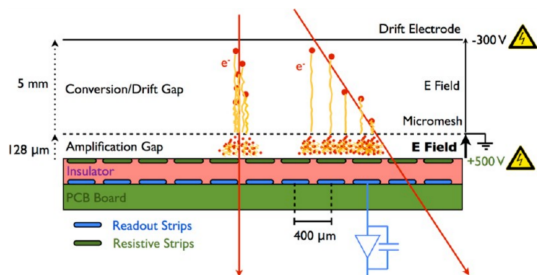


A triple-GEM detector: gain sharing between the foils improves the reliability of operation at high gains.



Recapitulation of the previous lecture

MicroMegas



- A MicroMegas can be considered as an RPC with an additional ionization and drift region.
- Advantage of the additional ionization region: higher primary charge than in an RPC.
- Disadvantage of the additional ionization region: A MicroMegas is slower than an RPC.

Recapitulation of the previous lecture

Time-Projection Chamber

- Time-projection chambers were developed in the 1980s to allow for charge particle detections with a very small amount of material along the track.

Leo 1993

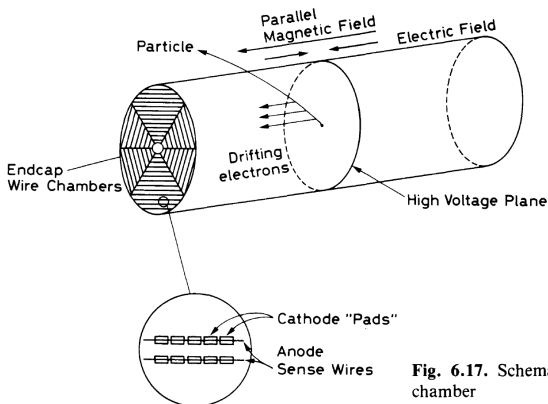


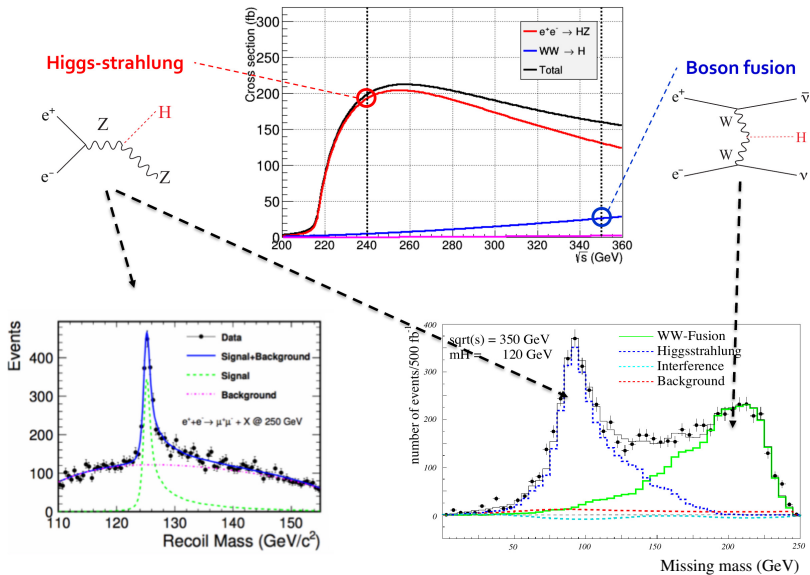
Fig. 6.17. Schematic diagram of a time projection chamber

- Modern TPCs use different detectors on the end caps, e.g. GEMs.
- Problem at the FCC-ee: Magnetic field must not exceed 2 T in order not to spoil the e^\pm beams. This leads to a reduced spatial resolution.

FCC-ee detector concepts

Recapitulation of the previous lecture

Higgs boson production at an e^+e^- Higgs factory

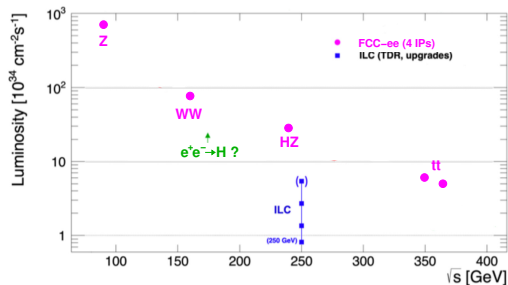


Recapitulation of the previous lecture

FCC-ee as Higgs factory plus EW and top factory

Higgs factory programme

- $2 \cdot 10^6$ HZ events (similar to the HL-LHC, but higher purity and selection efficiency) and 125,000 W^+W^- events.
- Precise measurements of Higgs couplings to fermions and bosons.
- Sensitivity to Higgs self-coupling at 2-4 σ level via loop diagrams.
- Unique opportunity to measure the electron coupling in $e^+e^- \rightarrow H$ at $\sqrt{s} = 125$ GeV.



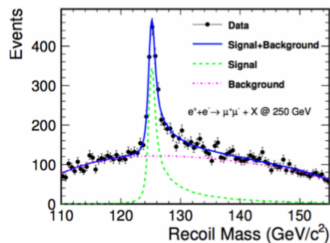
By changing the centre-of-mass energy of the collider the FCC-ee can also be operated as an electroweak and top quark factory.

- $\sim 100,000$ Z/s (1 Z/s at LEP).
- $\sim 10,000$ Ws/h (20,000 Ws in 5 years at LEP).
- $\sim 1,500$ top quarks/d.

Recapitulation of the previous lecture

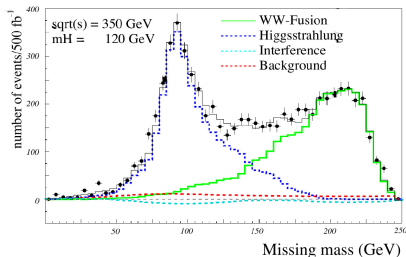
FCC-ee detector performance requirements

Higgs-strahlung



momentum resolution

WW fusion



jet energy resolution

$M_H = 125 \text{ GeV}$	SM BF
bb	56.1%
WW*	23.1%
gg	8.2%
$\tau\tau$	6.3%
ZZ*	2.6%
cc	2.9%
$\gamma\gamma$	0.2%
Z γ	0.15%
ss	0.1%
$\mu\mu$	0.02%

flavour tagging

Particle ID

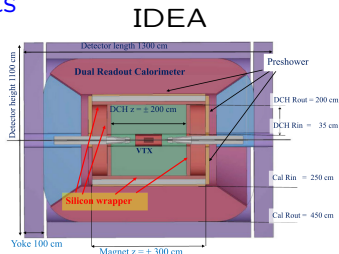
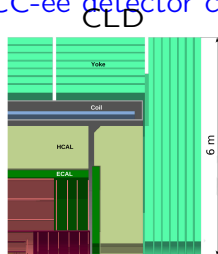
- $\frac{\delta p_T}{p_T} \sim 0.1\%$ for $p_T \sim 50 \text{ GeV}$ (to commensurate with beam energy spread).
- Jet energy resolution of $\frac{30\%}{\sqrt{E}}$ in multi-jet environment for Z/W separation.
- Superior impact parameter resolution for c and b tagging.

FCC-ee detector concepts

- 4 interaction zones at the FCC-ee allowing for 3 general-purpose detectors.
- 2 FCC-ee detector concepts, CLD and IDEA, presented in the FCC-ee CDR, + one new proposal. Designs are evolving.

Recapitulation of the previous lecture

FCC-ee detector concepts



Liquid Ar based ECAL

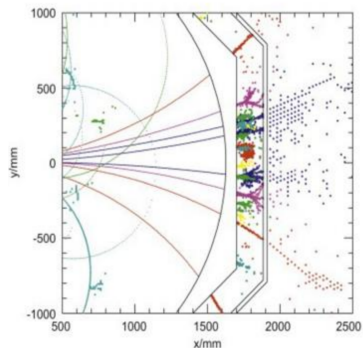


Subsystem	CLD	IDEA	LAr based ECAL
ID	Full silicon tracker	Silicon vertex detector, low X0 drift chamber with high-resolution PID via dE/dx , drift-chamber silicon wrapper	
ECAL	High-granularity silicon-tungsten	Dual-readout calorimeter	High-granularity lead/noble liquid ECAL
HCAL	High-granularity scintillator-steel	Lead-scintillating/Cherenkov fibres	To be specified
Muon	Instrumented steel-yoke with RPCs	μ Rwell chambers	To be specified
Magnet	Enclosing ID, ECAL, HCAL	MPGD/magnet coil/lead preshower	Enclosing ID

- Difficult to achieve required p_T resolution and PID performance with a full silicon tracker.
- Instrumented return yoke allows for momentum determination in the muon system.
- μ Rwell new technology with unclear advantages over RPCs.

Recapitulation of the previous lecture

Motivation for particle-flow hadron calorimeters



$$E_{jet} = E_{charged} + E_{\gamma} + E_{neutral\ hadrons}$$

Fraction 65% 26% 9%

- Particle-flow algorithms construct individual particles and estimate their energy/momentum in the best suited subdetector.
- Particle-flow algorithms require highly granular subdetectors including the calorimeters.
- Particle-flow algorithms use the granularity to separate the neutral from the charged contributions and exploit the tracking system to measure charged particle momenta precisely.

Charged track resolution	$\frac{\delta p}{p} \lesssim 0.1\%$
γ energy resolution	$\frac{\delta E}{E} \sim \frac{12\%}{\sqrt{E}}$
Neutral hadron energy resolution	$\frac{\delta E}{E} \sim \frac{45\%}{\sqrt{E}}$

Recapitulation of the previous lecture

Dual read-out based calorimeters

Starting idea

- Use scintillators to detect/measure the energy depositions of shower particles.
- Use Čerenkov light to measure the speed of light of relativistic charged shower particles.

Scintillation signal S and Čerenkov signal C

$$S = E \left[f_{em} + \frac{1}{(e/p)_S} (1 - f_{em}) \right],$$
$$C = E \left[f_{em} + \frac{1}{(e/p)_C} (1 - f_{em}) \right].$$

If one knows $(e/p)_S$ and $(e/p)_C$, one gets

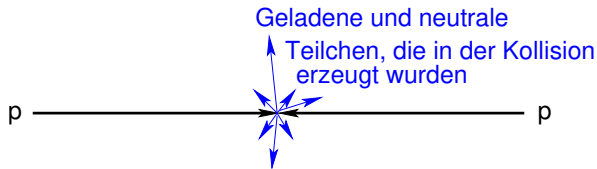
$$E = \frac{S - \chi \cdot C}{1 - \chi}$$

with

$$\chi := \frac{1 - (p/e)_S}{1 - (p/e)_C}$$

which is independent of E and the particle nature.

Recapitulation of important topics



Particles which can be produced in a pp collision

Leptonen

- Neutrinos: stable, but only weakly charged. \Rightarrow No interaction leading to a measurable electronic signal in the detector components.
- Electrons: stable, electrically charged. \Rightarrow Electronic signals in the detector components.
- Muons: unstable, but ultrarelativistic, hence longlived in the laboratory system that they do not decay in the detector; electrically charged. \Rightarrow Electronic signals in the detector components.
- τ leptons: unstable. \Rightarrow Have to be detected via their decay products.

Further final state particles

Hadrons

- In the pp collision quarks and gluons are formed. Due to the quark confinement, we do not see quarks and gluons in the detector, by so-called “hadron jets” which are created from the initial quarks and gluons.
- Special role of two types of quarks:
 - b quarks build longlived b hadrons which makes it possible to identify b quark jets.
 - t quarks are so shortlived that they cannot build hadron. They can be identified by the decay $t \rightarrow Wb$.
- Jets contain mainly the lightest mesons, namely π^+ , π^- , π_0 which are quasistable due to the large Lorentz boost.

Photons

Photons are stable. They are electrically neutral, but can create electromagnetic showers in the detector material which can be detected.

Two effects in the passage of charged particles through matter:

- Energy loss.
- Deflection from the original trajectory.

Processes causing energy loss and deflection

- Inelastic scattering off atomic electrons in the traversed material.
- Elastic scattering off the nuclei of the traversed material.
- Emission of Čerenkov radiation.
- Nuclear reactions.
- Bremsstrahlung.

The radiation field of an accelerated charge is proportional to its acceleration a_{charge} . The energy of the radiation is proportional to $|\vec{E}|^2$ which is proportional to $a_{charge}^2 = \left(\frac{F}{m}\right)^2 \propto \frac{1}{m^2}$. Hence bremsstrahlung is only important for electrons, but not for heavy charged particles.

Energy loss of heavy charged particles

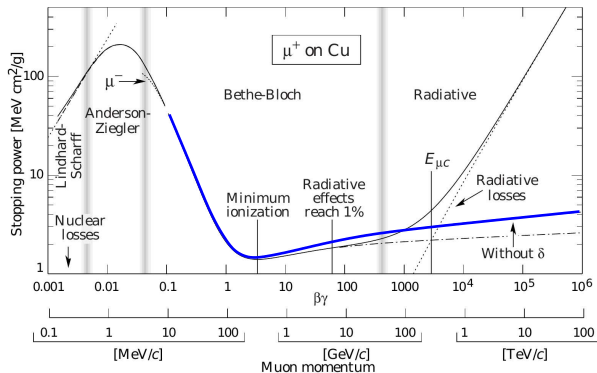
Heavy charged particles lose energy by excitation and ionization of atoms. The energy loss is described by the **Bethe-Bloch formula**:

$$-\frac{dE}{dx} = \frac{4\pi n z^2}{m_e c^2 \beta^2} \cdot \left(\frac{e^2}{4\pi\epsilon_0} \right)^2 \cdot \left[\ln \left(\frac{2m_e c^2 \beta^2}{I(1 - \beta^2)} - \beta^2 \right) \right];$$

$\beta = v/c$: Velocity of the particle. E : Energy of the particle.

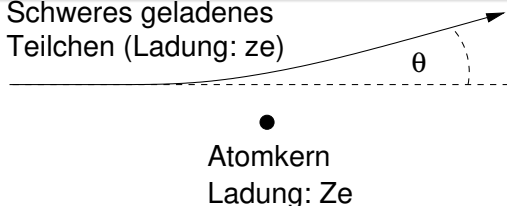
z : Charge of the particle. e : Elementary charge. n : Electron density of the material.

I : Average excitation potential of the material.



Multiple scattering

Schweres geladenes
Teilchen (Ladung: ze)

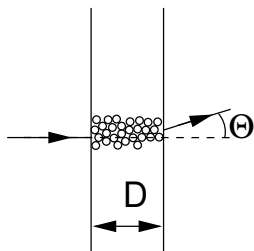


Scattering off a single nucleus:

$$\theta = \frac{\Delta p}{p} \propto \frac{z \cdot Z}{p}$$

$$\langle \theta \rangle = 0, 0 \neq \theta_0^2 := \text{Var}(\theta) \propto \frac{z^2 \cdot Z^2}{p^2}$$

Scattering off many nuclei:



$$\langle \Theta \rangle = 0$$

$$\Theta_0^2 := \text{Var}(\Theta) = \sum_{\text{collisions}} \theta_0^2 \propto D \cdot z^2 \cdot Z^2 p^{-2}$$

Hence $\Theta_0 \propto \frac{\sqrt{D}}{p}$.

The exact treatment gives

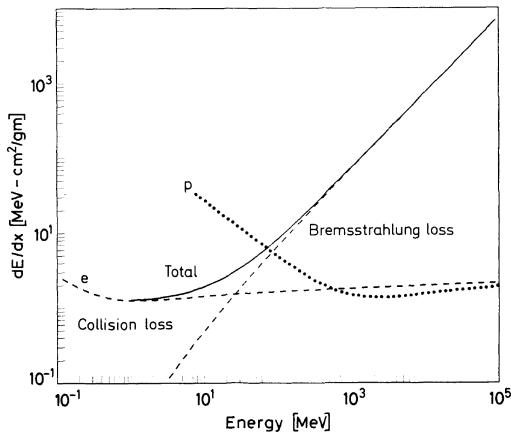
$$\theta_0 := \frac{13,6 \text{ MeV}}{E} \sqrt{\frac{d}{X_0}}$$

where the term under the square root happens to be equal to the radiation length X_0 of the material.

Energy loss of electrons (and positrons)

m_e is so small that the acceleration the electrons/positrons experience in collisions with atomic nuclei is so large that bremsquanta can be emitted.

$$\left. \frac{dE}{dx} \right|_{e^\pm} = \left. \frac{dE}{dx} \right|_{\text{collisions}} + \left. \frac{dE}{dx} \right|_{\text{Bremsstrahlung}}$$



Critical energy E_k

$$\left. \frac{dE}{dx} \right|_{\text{collisions}} (E_k) = \left. \frac{dE}{dx} \right|_{\text{Brems.}} (E_k).$$

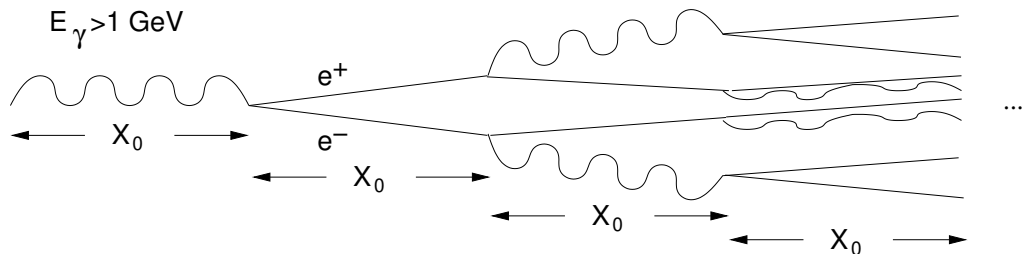
$E_k \approx \frac{800 \text{ MeV}}{Z+1/2}$, such that bremsstrahlung is the dominant process for $E_{e^\pm} > 1 \text{ GeV}$.

Dominant processes

1. Photoelectric effect.
2. Compton scattering
3. e^+e^- pair production

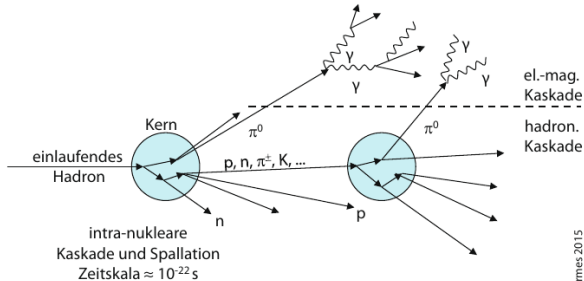
⇒ A beams of photons does not lose energy when passing through matter, but intensity because all three processes remove photons from the beam.

Electron photon showers



- After a distance $n \cdot X_0$: 2^n particles with energy $E_n \approx \frac{E_\gamma}{2^n}$.
- End of the cascade (shower), if $E_n = E_k$: $n = \frac{\ln \frac{E_\gamma}{E_k}}{\ln 2}$.
- Shower length: $n \cdot X_0 = X_0 \cdot \frac{\ln \frac{E_\gamma}{E_k}}{\ln 2}$.
- Transverse size of the shower independent of E_γ :
 $L_\perp \approx 4R_M = 4X_0 \frac{21,2 \text{ MeV}}{E_k}$.

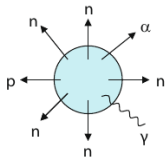
Hochenergie-Kaskade



Kolanoski, Wermes 2015

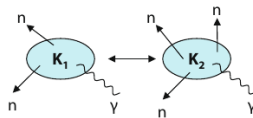
Deaktivierung des Kerns

Zeitskala $\geq 10^{-18}$ s



Evaporation

oder

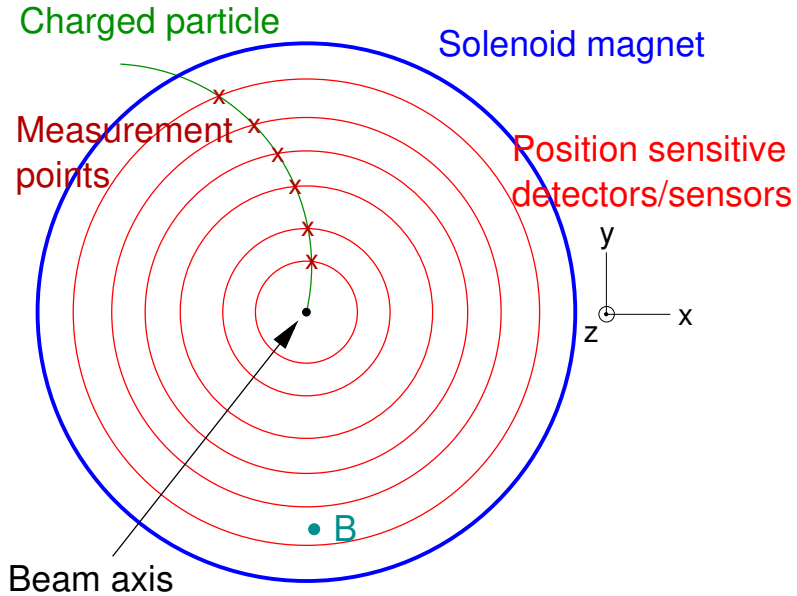


Spaltung

Similar behaviour like electromagnetic showers:

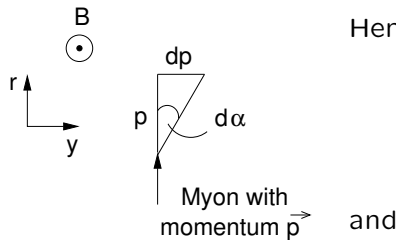
- Shower length proportional to $\lambda_A \approx 35 \text{ g cm}^{-2} \frac{A^{1/3}}{\rho} \gg X_0$.
- Transverse size independent of the energy of the primary hadron: λ_A .
- But much stronger variations of the shower size than in case of electromagnetic showers.

Basic structure of a particle detector at a hadron collider



Charged particle trajectories in the inner detector

$$d\alpha = \frac{dp}{p} = \frac{qvBdt}{p} = \frac{q}{p}B \underbrace{vdt}_{=ds=dr} = \frac{q}{p}Bds.$$



$$\alpha(r) \approx \frac{q}{p} \int_{r_0}^r B(s) ds$$

$$y(r) = \int_{r_0}^r \alpha(r') dr' = \frac{q}{p} \int_{r_0}^r \int_{r_0}^{r'} B(s) ds dr'.$$

Beispiel. $p = 1 \text{ GeV}$. $r_0 = 0$. $B = 2 \text{ T}$.
 $\alpha(10 \text{ cm}) = 60 \text{ mrad}$. $y(10 \text{ cm}) = 3 \text{ mm}$.
 $\alpha(1 \text{ m}) = 0,6 \text{ rad}$. $y(1 \text{ m}) = 30 \text{ cm}$.

- Deflection angle at distance r from the pp interaction point:

$$\alpha(r) = \frac{q}{p} \int_0^r B ds$$

- Total deflection angle: $\alpha := \alpha(r_{max})$ (r_{max} radius of the inner detector).
- Error propagation:

$$\delta\alpha = \frac{|q|}{p^2} \int_0^{r_{max}} B ds \cdot \delta p = \alpha \cdot \frac{\delta p}{p} \Leftrightarrow \frac{\delta p}{p} = \frac{\delta\alpha}{\alpha}$$
$$\frac{\delta p}{p} = \frac{\delta\alpha}{\frac{|q|}{p} \int_0^{r_{max}} B ds}$$

$$\frac{\delta p}{p} = \frac{\delta \alpha}{\frac{|q|}{p} \int_0^{r_{max}} B ds}$$

- Contributions to $\delta \alpha$

$$\begin{aligned} \delta \alpha &= \sqrt{(\delta \alpha_{mult. \text{ scatt.}})^2 + (\delta \alpha_{det. \text{ res.}})^2} \\ &= \sqrt{\left(13,6 \text{ MeV} \sqrt{\frac{D}{X_0}}\right)^2 + (\delta \alpha_D)^2} \end{aligned}$$

Hence

$$\frac{\delta p}{p} = \frac{13,6 \text{ MeV} \sqrt{\frac{D}{X_0}}}{|q| \int B ds} \oplus \frac{\delta \alpha_D}{|q| \int B ds} \cdot p$$

- ⇒ Best possible momentum given by the ratio of multiple scattering and the magnetic field integral.
- ⇒ High momenta (small values of α): Momentum resolution determined by the ratio of the spatial resolution of the detector and the magnetic field integral. The momentum resolution degrades with increasing p .

Requirements

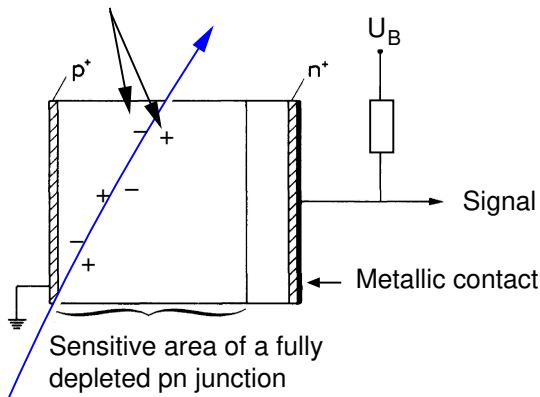
- Little amount of detector material to minimize the multiple scattering contribution to the momentum
- High position resolution to maximize the momentum resolution for highly energetic particles.
- High granularity to be able to separate tracks of individual particles for high particle densities.
- Radiation hardness.

Used detector types

- Originally gaseous ionization detectors were used. These have a small material budget, but limited spatial resolution, granularity, and radiation hardness.
- Nowadays: semiconductor detectors which offer high spatial resolution and high granularity.

Basic principle of a semiconductor detector

Liberated charge carriers which are pulled by the electric field towards the contact



Ionizing particle

In order to prevent the creation of an ohmic contact with a depletion zone extending far into the semiconductor, contact surfaces with highly doped layers are used.

Nomenclature

Passive medium: Material in which the shower develops.

Aktive medium: Material in which the electronically detectable signals of the shower particles are created.

Two types of calorimeters

- Homogeneous calorimeters, in which the active material also serves as passive material.
- Inhomogeneous calorimeters or sampling calorimeters with alternating layers of active and passive materials.

Hadron calorimeters are always sampling calorimeters in order to limit their size. There are homogeneous and inhomogeneous electromagnetic calorimeters.

Energy resolution

- The energy measurement in a calorimeter consist of the detection of the shower particles. The measured energy is proportional to the number of detected shower particles N leading to $\frac{\delta E}{E} = \frac{\delta N}{N} = \frac{1}{\sqrt{N}}$.
- In a real calorimeter contributions to the energy resolution from detector noise and mechanical and electronic non-uniformities must be taken into account:

$$\frac{\delta E}{E} = \frac{a}{\sqrt{E}} \oplus \underbrace{\frac{b}{E}}_{\text{El. noise}} \oplus \underbrace{c}_{\text{Non-uniformities}}$$

Linearity

Not only $\frac{\delta E}{E}$ is important, but also that the measured signal depends linearly on E .

- Scintillation counters are important detectors for the active part of a calorimeter.
- Material which emit a small flash of light when hit by radiation
 - **Important properties of the signal of a scintillation counter:**
 - Above a certain minimum energy deposition, **the amount of scintillation light is proportional to the deposited energy** (in good approximation).
 - **Fast response**, i.e. the light signal is created a short time after the energy deposition.
- **Liquid argon** is also used as **active medium** in calorimeters.
- In liquid argon the noble gas has such a high density that the shower particle liberate many electrons by ionization.
- In order to collect these electrons the liquid argon is enclosed by two electrodes at high voltage.

See lectures on Jan. 8!

Many thanks for your participation in the course!
I would be happy to meet you for the second part of the lecture in the
summer semester.